Available online at www.sciencedirect.com

SciVerse ScienceDirect

Journal of the European Ceramic Society 32 (2012) 777–785

www.elsevier.com/locate/jeurceramsoc

Preparation and characterization of ZTA bioceramics with and without gradient in composition

Claudia Ortmann [a,*], Thomas Oberbach [a], Hannes Richter [b], Petra Puhlfürß [b]

[a] *Mathys Orthopaedie GmbH, 07646 Moersdorf, Germany*

[b] *IKTS – Fraunhofer Institut für Technische Keramik und Systeme, Institutsteil Hermsdorf, 07629 Hermsdorf, Germany*

Received 3 June 2011; received in revised form 11 October 2011; accepted 1 November 2011
Available online 25 November 2011

Abstract

Properties and proof of suitability of homogeneously and graded ZTA bioceramics with various Y_2O_3 stabilized zirconia contents were investigated. Therefore porous alumina was infiltrated with different amounts of Y_2O_3 doped ZrO_2 precursors. At homogeneously infiltrated samples biaxial flexural strength and wear behavior were investigated (ISO 6474). Subsequently, at hip joint heads the static fracture strength was determined (ISO 7206-10). Materials ranging from approx. 4 to 20 wt% Y_2O_3 stabilized zirconia were characterized relative to the sinter density, the microstructure, the phase composition and the dispersion of the stabilized zirconia phase. Bioceramics showed high sinter density, fine microstructures, excellent wear property and significantly increased biaxial flexural strength. A 41% increase in strength through the formation of Y_2O_3 stabilized zirconia gradient in the conical bore of the heads was reached. Low compressive stresses in cone of this heads were found.

ZTA bioceramics are potentially suitable for use as hip replacement components.

Keywords: Biomedical application; Composites; ZrO_2–Al_2O_3; Mechanical properties; Wear resistance

1. Introduction

Since bioceramic implant materials such as aluminum oxide (Al_2O_3) and partially stabilized zirconium oxide (Y_2O_3 stabilized zirconia) have been used for load-bearing components of hip replacements, mechanical strength and wear have been the focus of material development and characterization. Combined with other material properties, such as microstructure, sinter density and purity of the material, the required level of implant safety is achieved and can be increased where necessary by the further development of the ceramic materials.[1,2] In this way, during the last few years various dispersion ceramics like zirconia toughened alumina (ZTA) and alumina toughened zirconia (ATZ) with a homogeneous microstructure and consisting of the components Al_2O_3 and Y_2O_3 stabilized zirconia have been developed by various manufacturers.[3,4] Electrophoretic deposition (EPD) has been used to prepare ceramic Al_2O_3/ZrO_2 graded composites in laboratory scale. That method requires large equipment related efforts according to EPD set-up. Furthermore well prepared longtime stable ceramic composite suspensions are necessary.[5,6] Another EPD method was used to prepare functionally graded materials (FGM) with several layers resulting in an alumina–ZTA composite. Here step by step the ZTA composition changed from alumina to 14 vol% ZrO_2 over 22 vol% ZrO_2 to 30 vol% ZrO_2 and back.[7] Another possibility for combining the excellent mechanical and tribological properties of Al_2O_3 and Y_2O_3 stabilized zirconia is to infiltrate a fluid Y_2O_3 doped zirconia precursor in a porous Al_2O_3 matrix.[8,9] Chemical vapor infiltration processes require a high degree of outlay with regard to apparatus.[10] The use of fluid precursors presents a simple alternative.[11,12] Here the process can be controlled so that both homogeneous and graded components can be created, as could be shown from a range of material combinations.[8,13–15]

In addition to the production of homogeneous Y_2O_3 stabilized zirconia–alumina dispersion ceramics (ZTA) through the infiltration of a fluid precursor in a porous Al_2O_3 matrix, in this study graded ZTA-ceramics are also produced and characterized using this simple technology. Artificial ceramic hip joint heads are prepared by this method for the first time. The graded material distinguishes itself by both a graded index of the chemical

* Corresponding author.
E-mail address: claudia.ortmann@mathysmedical.com (C. Ortmann).

0955-2219/$ – see front matter © 2011 Elsevier Ltd. All rights reserved.
doi:10.1016/j.jeurceramsoc.2011.11.002

composition – Al_2O_3 ratio to Y_2O_3 stabilized zirconia – and through a particle size graded index.

2. Materials and methods

2.1. Material

In order to investigate the ZTA bioceramics, various geometric test samples were prepared. The strength of the material was determined on b-discs (discs for biaxial bending strength test) with different contents of Y_2O_3 stabilized zirconia (4, 8, 12 and 20 wt%) but homogeneous compositions. To assess wear behavior, ring-on-disc (rod) samples were produced with an analogue composition. The preparation of hip joint heads (head type 28L) was subsequently carried out to determine the static fracture load on the components. Here both homogeneous composition and graded composition were implemented in the component.

2.1.1. Infiltration solutions

Six different, nano disperse suspensions and/or solutions were used for the infiltration tests:

(a) Ceramic slips were manufactured from Y-TZP powder (VP 3-YSZ Degussa, average primary particle size < 30 nm, manufacturer information) using milling and dispersion. The particle sizes achieved through this were approx. 100 nm determined by laser particle size analysis.
(b) Through the complete hydrolysis of metal alcoholates (zirconium–n-propoxide, yttrium(III)–isopropoxide; Sigma–Aldrich) in water and subsequent precipitation with HNO_3, clear, aqueous colloidal Y–ZrO_2 sols with particle sizes of 4 nm were created.
(c) Through only partial hydrolysis and subsequent acid catalyzed polycondensation of the metal alcoholates in organic solvents (n-propoxide; Sigma–Aldrich), clear, low viscosity polymer Y–ZrO_2 sols were produced. For the metal polymer species resulting from this process, no particle sizes could be calculated.
(d) Through the reaction of Y- and Zr-alcoholate (zirconium–n-propoxide, yttrium(III)–isopropoxide; Sigma–Aldrich) with acetone (Fluka), clear, low viscosity solutions with metal organic aggregates were created.
(e) Pure metal alcoholates were mixed and diluted with n-propyl alcohol (Fluka) for infiltration tests.
(f) Solutions from Y_2O_3 and ZrO_2 salts ($Y(NO_3)_3{\cdot}6H_2O$, Merck, $ZrO(NO_3)2{\cdot}H_2O$; Sigma–Aldrich) were produced. Dissociated salts were found in these aqueous, low viscosity solutions so that one could assume the ionic diameter of hydrated metal ions for the "particle size".

With the various initial solutions, the porous matrixes of uniform geometric form (b-discs) described hereafter were completely infiltrated – means dip infiltration until saturation of matrix – once in a 10 min immersion process. After 12 h air drying, 5 h at 120 °C drying in air and thermal treatment 1 h at 1000 °C in air, the solution with which the highest content of Y_2O_3 stabilized zirconia in the matrix could be created was gravimetrically calculated. All further infiltration tests were carried out with this solution. The composition of the respective solutions was chosen that stabilization of the ZrO_2 with 3 mol% Y_2O_3 was achieved in the bioceramics.

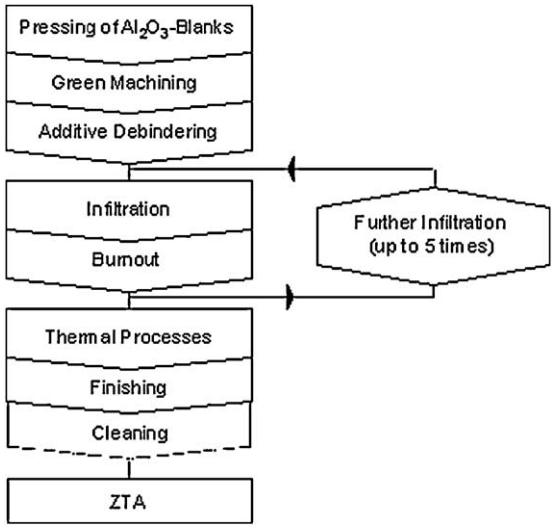

Fig. 1. Diagram showing the production of samples.

2.1.2. Matrix–matrix infiltration-dispersion ceramics

Porous thermal pretreated (1 h at 1000 °C in air) Al_2O_3 ceramics served as a matrix. Alumina matrix material evidenced by 2.38 g/cm^3 density, 40% open porosity and a median pore diameter of 130 nm. The production and further infiltration of these are represented schematically in Fig. 1 and explained below and in 16.

After every kind of infiltration samples were dried 1 h in air at room temperature, 5 h at 120 °C in air and 1 h at 1000 °C in air. This process resulted in transformation of the infiltrated precursor in Y_2O_3 stabilized zirconia inside the alumina matrix. After the final infiltration cycle, the samples were sintered at 1500 °C in a H_2 atmosphere and redensified at 1450 °C and 1000 bar at argon atmosphere in a hot isostatic process (HIP). Subsequently, the finishing of the discs and rod-samples was carried out through grinding, lapping, polishing and followed by cleaning. Finishing of hip joint heads ended after the grinding of the conical bore of the head and the outer surface.

Table 1 summarizes the number of generated samples as there are alumina reference material and different dispersion ceramics made of alumina and Y_2O_3 stabilized ZrO_2 were prepared.

The porous b-disc matrixes and the rod-sample matrixes were completely infiltrated – means dip infiltration until saturation of matrix – with the solutions of the dissociated salts. During process, they were several times (up to 5 times) dip infiltrated for 10 min using salt solutions (type f).

The hip joint head matrixes were infiltrated on the one hand 5 times completely (dip infiltration until saturation of matrix with solution of dissociated) and on the other partially resulting in a gradient composition. Here only the conical bore of the hip joint head is filled with solution of dissociated salt for 3 times – 12 min, 5 min and 2 min.

Table 1
Overview of the tested samples prepared with salts.

Sample name	Sample form	Material	Number of infiltrations	Depth of infiltration
0	b-disc	Al_2O_3 (Bionit®)	–	–
I	b-disc, rod-samples	$Al_2O_3 + Y_2O_3$ stabilized ZrO_2	1×	Fully infiltrated
II	b-disc, rod-samples	$Al_2O_3 + Y_2O_3$ stabilized ZrO_2	2×	Fully infiltrated
III	b-disc, rod-samples	$Al_2O_3 + Y_2O_3$ stabilized ZrO_2	3×	Fully infiltrated
IV	b-disc, rod-samples	$Al_2O_3 + Y_2O_3$ stabilized ZrO_2	4×	Fully infiltrated
V	b-disc	$Al_2O_3 + Y_2O_3$ stabilized ZrO_2	5×	Fully infiltrated
A	hip head	Al_2O_3 (Bionit®)	–	–
B	hip head	$Al_2O_3 + Y_2O_3$ stabilized ZrO_2	5×	Fully infiltrated
C	hip head	$Al_2O_3 + Y_2O_3$ stabilized ZrO_2	3×	Partially infiltrated

2.2. Methods

The calculation of the Y_2O_3 stabilized zirconia content achieved was carried out gravimetrically on the b-discs infiltrated with the various solutions. By means of measuring the sample geometry, the shrinkage was calculated and furthermore, the density of all of the sintered samples was determined through hydrostatic weighting. High fracture strength and resistance to wear (no abrasion particles generated in the body) are indispensable characteristics for the implant. These are the foundations for the safety of a ceramic implant and a long service life and are therefore the focal point of the investigations. The determination of the biaxial flexural strength was carried out on 30 discs per series. The static fracture load test on the hip joint head was carried out on 10 parts per material composition and for the wear screening, 5 ring on disc pairings (individual pairings) were carried out per composition. The ring on disc test was performed under the following conditions:

Axial force	1500 N
Rotation frequency	1.0 Hz
Rotational angle	±25°
Test fluid	25% serum
Test period	100 h
Number of pairings	5

Wear trace on the disc was measured at the end of the test by using a surface scanning device (Mitutoyo Surftest SJ-401). The wear volume was calculated on the basis of the volumes and the density of the respective material composition. The biaxial flexural strength and the wear behavior test were carried out in accordance with ISO 6474 and static fracture load on the hip joint heads was done using a fracture strength testing machine Inspekt 300-1 in accordance with ISO 7206-10.[17,18] The values determined from measuring the biaxial flexural strengths were evaluated using Weibull statistics together with the maximum likelihood parameter method.

The calculation of the phase content was carried out on the solidified product of dried and calcinated (1000 °C) salt solution (solution "f") using XRD. Furthermore, using a GE Seifert 3003TT with 1 mm fox optic combined with Rietveld refinement (BGMN "AutoQuan"), the radiographical phase content – especially the monocline amount – of the created bioceramics was calculated prior to and following the wear test, on one disc of the corresponding test series from the ring on disc test. Determination of residual stress distribution on fractured surfaces at graded composite hip head (series C, 3 times partially infiltrated) and Bionit® (alumina) hip head were carried out at that instrument too. The angle range between 135° and 138° was measured and stresses were calculated by $\sin^2$ theta method. The microstructure and the dispersion of the Y_2O_3 stabilized zirconia in the respective matrix (from inside cone radial to surface) were assessed using REM/EDX. The investigations were carried out using a field emission electron microscope ULTRA 55 plus from Zeiss.

3. Results and discussion

3.1. b-Discs

After the simple, complete infiltration of the discs, significant differences were found in the Y_2O_3 stabilized zirconia content depending on the infiltration solution used (Fig. 2). The lowest Y_2O_3 stabilized zirconia loading of 0.1 wt% was achieved with ceramic slips (solution "a"), the highest loading of 4.3 wt% was achieved with Y_2O_3 doped ZrO_2 salt solutions (solution "f"). As clear improvements of the mechanical material properties were only expected with sufficiently high Y_2O_3 stabilized zirconia loading, the salt solutions were selected for all further infiltration tests.

For the pure salt solutions (solution "f"), after drying and calcination at 1000 °C, only the peaks for tetragonal ZrO_2 could be found in the X-ray diffractogram (Fig. 3). The ZrO_2 was then successfully stabilized with Y_2O_3, which enables the deduction of a successful mixture of both components at a molecular level.

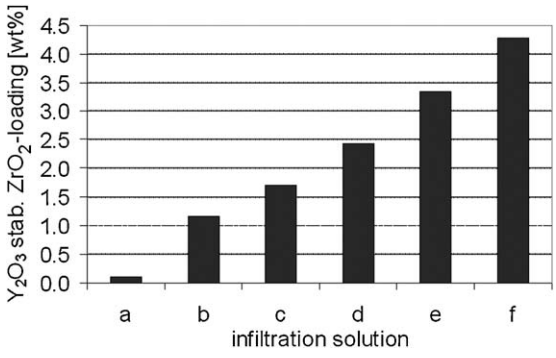

Fig. 2. Y_2O_3 stabilized zirconia loading on simple, fully infiltrated Al_2O_3 disc matrixes for various infiltration solutions.

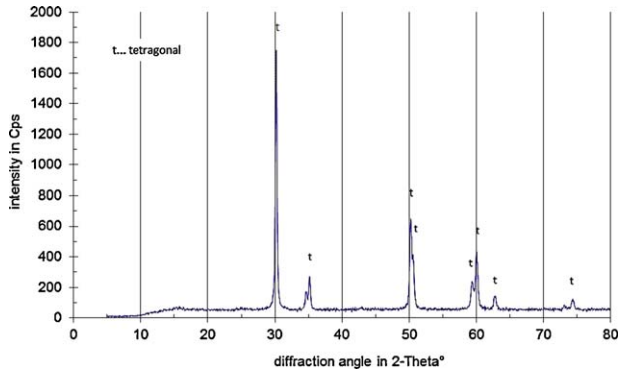

Fig. 3. X-ray diffractogram of a mixture of Zr and Y saline solutions after drying and calcination at 1000 °C.

For multiple, complete infiltration of porous Al_2O_3 discs with the Y_2O_3 stabilized zirconia salt solution, after the conclusive thermal treatment an almost linear independency of the Y_2O_3 stabilized zirconia loading from the number of infiltration steps was determined (Fig. 4). After infiltration occurred 5 times, around 20 wt% Y_2O_3 stabilized zirconia was separated in the Al_2O_3 matrix. With increasing Y_2O_3 stabilized zirconia proportion, the sinter density of the samples increased from 3.89 g/cm^3 for non-infiltrated Al_2O_3 to 4.23 g/cm^3 for Al_2O_3 which had been infiltrated 5 times with 20 wt% Y_2O_3 stabilized zirconia, whereby a linear independency of the sinter density from the Y_2O_3 stabilized zirconia content was shown (Fig. 4). Furthermore, it was found that all samples had at least 99% theoretical density.

One Al_2O_3 reference (Bionit®) and 4 various Y_2O_3 stabilized zirconia contents (each with 30 b-discs) were loaded using the Biaxtest until breakdown. With a constant characteristic lifetime of 63%, with each infiltration step an increase of the burst load from 387 MPa for pure Al_2O_3 to 589 MPa for Al_2O_3 infiltrated 5 times with 20 wt% Y_2O_3 stabilized zirconia was able to be established (Fig. 5). The Weibull modulus dropped slightly here, but remained in the technically interesting area of >10 (Table 2) even for samples which had been infiltrated 5 times.

3.2. Rod-samples

The results of the wear screening tests (Fig. 6) showed a consistent abrasion of around 0.18 mg independent of the Y_2O_3 stabilized zirconia loading. This corresponds with the value of 0.19 mg calculated in the previous tests for the standard material Al_2O_3 (Bionit®).[19,20]

To calculate the influence of the phase composition, especially on monocline amount, through the wear test, one sample was examined before and after wear exposure from every test series using XRD (Fig. 7). The total ZrO_2 contents corresponded approximately with the gravimetrically determined values. The gravimetrically determined Y_2O_3 stabilized zirconia contents showed that particular values were higher compared to the X-ray graphical values, as Y_2O_3 was included in the measurement. Only an extremely low monocline ZrO_2 proportion of 1.1–2.8%, exclusively in relation to 100% ZrO_2 proportion, was found before the wear test. After the wear

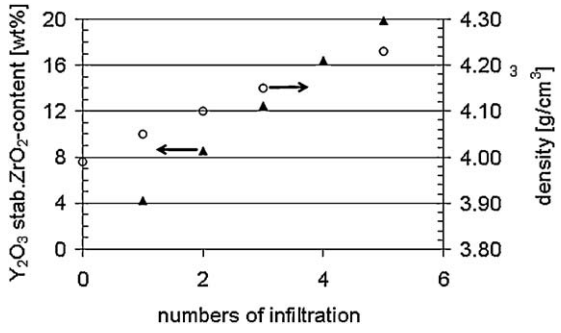

Fig. 4. Y_2O_3 stabilized zirconia loading and density of salt infiltrated Al_2O_3 matrixes after sintering dependent of the number of infiltration steps.

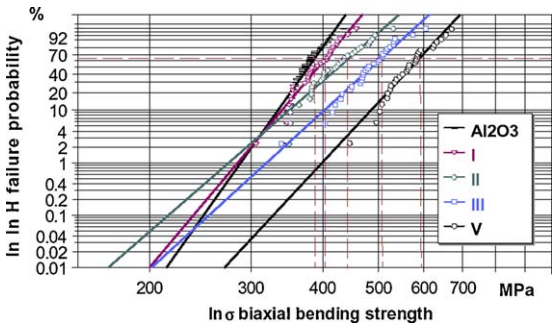

Fig. 5. Weibull plot of test series with various Y_2O_3 stabilized zirconia loading – in comparison with Table 1 – (biaxial bending strength test in accordance with ISO 6474).

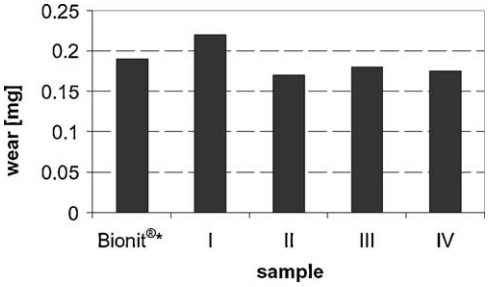

Fig. 6. Wear amount of test series with various Y_2O_3 stabilized zirconia contents (ring-on-disc, *value for Al_2O_3 – Bionit® – from previous investigations [19,20]).

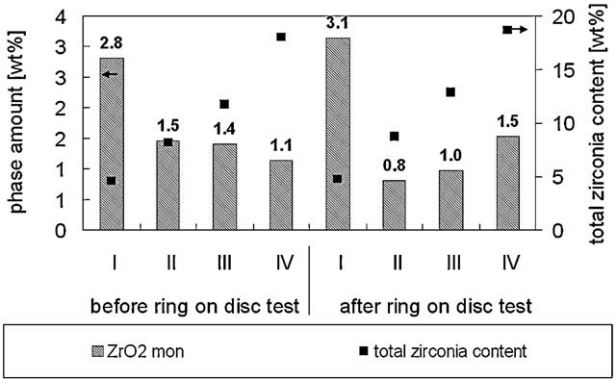

Fig. 7. Phase composition of the ZrO_2 proportion in the variously composed ZTA series prior to and after exposure to wear (ring-on-disc).

Table 2
Statistical results of the biaxial bending strength tests for test series with various Y_2O_3 stabilized zirconia loading.

Sample	Al_2O_3 Bionit®	I	II	III	V
Characteristic lifetime (failure probability 63%) [MPa]	387	404	444	505	589
Weibull modulus	15.6	13.1	9.6	10.0	11.8

tests, the total ZrO_2 proportion and the ratio of the monocline modification remained almost unchanged. The superficial wear loading did not have any significant influence on the ZrO_2 phase composition. At a sample with about 8 wt% ZrO_2 in alumina the transformability was estimated as the difference between the monocline amount in relation to 100% ZrO_2 of a polished (1.2%) and a fracture surface (12%) and resulted in (10.8 ± 7)% transformability. The standard deviation is as high because of the roughness of fracture surface.

3.3. Hip heads

Porous Al_2O_3 hip joint head matrixes (Bionit®) were infiltrated 5 times completely (in the case of samples B) or 3 times on one side (series C – see Table 1) and sintered.

For series B, an Y_2O_3 stabilized zirconia content of 17.22% was calculated gravimetrically (Table 3). This value was somewhat lower than that for the fully infiltrated b-discs of series V. The cause of this was an incomplete salt infiltration up to the core of the hip joint ball that was visible to the naked eye from the section (Fig. 8). Using EDX, a nearly homogeneous ZrO_2 loading was able to be found up to a depth of approx. 2 mm based on both infiltration fronts (conical bore and ball surface) (Figs. 8 and 9). In these areas, the ZrO_2 content was around 15 wt%. In the case of a larger distance from the infiltration front, the ZrO_2 loading decreased to a minimum value of 3 wt% ZrO_2. Hip joint balls infiltrated on one side (sample C) showed a low total Y_2O_3 stabilized zirconia content of 5.28 wt% as expected (Table 3). On the cross section, the infiltration area of approx. 5.5 mm was clearly visible starting from the cone (Fig. 8). Using EDX analyses, a decrease in the ZrO_2 content within this area from approx. 12 wt% to 0 wt% was determined (Fig. 9). Furthermore at this sample at 3 places a series of EDX measurements radial from

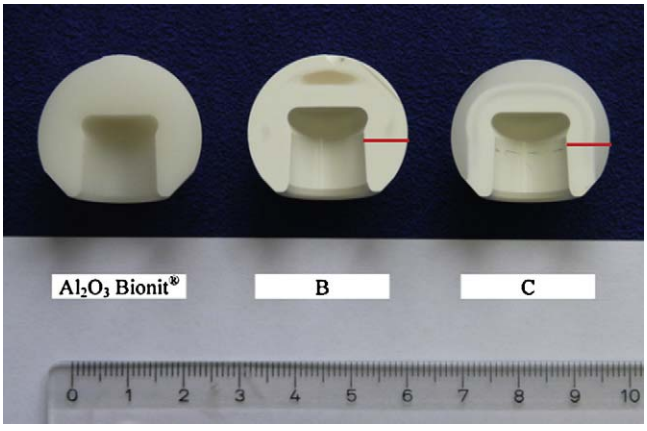

Fig. 8. Section of the samples Al_2O_3 (Bionit®), series B and series C after sintering.

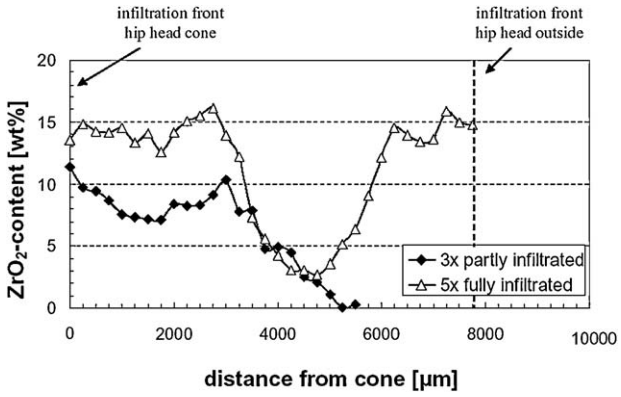

Fig. 9. Local ZrO_2 dispersion, one sample each from series B and C (EDX analysis with defined distance from the conical bore of the hip joint head).

the cone to the outer surface in a line were performed (Fig. 10). Every profile showed the same gap between 500 and 3000 µm from cone. The local zirconia minimum at this area was 9 wt% ZrO_2. It may result from infiltration step by step and should be avoided by improved infiltration technique.

The residual stress distribution at a one side infiltrated graded hip head (fracture surface) showed relative low compressive (−42 MPa) stress in the area with the highest content of Y_2O_3 stabilized ZrO_2 (Fig. 11). With decreasing Y_2O_3 stabilized zirconia amount the compressive stress decreased too and changed inside the hip joint head in low tensile stress that is not observed on alumina hip head showed nearly no residual stress distribution (Fig. 11). The detected stresses on fracture surfaces were low compared to Novak who investigated polished surfaces of layer by layer prepared samples.[7] Polishing could have influenced the stress distribution of samples to higher stress values. Until now it can pointed out that because of the compressive stresses in partially infiltrated hip heads the strength could be influenced positive but not in a high value (also discussed

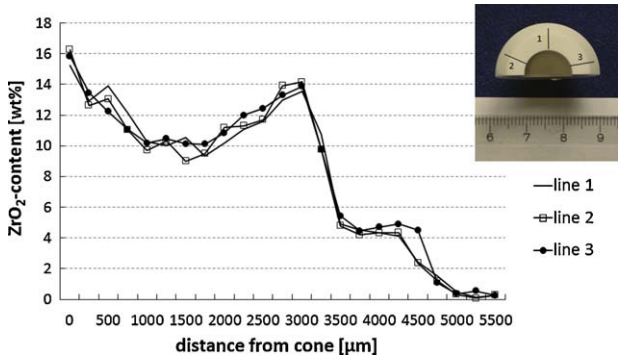

Fig. 10. EDX line scan for determination of radial ZrO_2 dispersion in 3 times partially infiltrated hip joint head (series C).

Table 3
Density and Y_2O_3 stabilized zirconia content on infiltrated and sintered Al_2O_3 hip joint balls.

Sample	Number of infiltrations	Y_2O_3 stabilized zirconia content (gravimetric) [%]	Density [g/cm^3]
A (Bionit®)	–	–	3.98
B	5 times fully	17.22	4.27
C	3 times partially	5.28	4.06

later on in accordance with shrinkage). Other mechanisms like grain size refinement (microstructure) and dispersion as itself (transformation toughening), contribute to strength increase also and probably more. In case of complete infiltrated hip heads which were not investigated according to their stress distribution the assumption is made that because of the gap in Y_2O_3 stabilized ZrO_2 content inside the sample the microstructure could have been damaged in accordance with different shrinkage and changing stress distribution. From the results of the gradient material compressive stresses on outer surface and inside cone are expected. But changing composition connected with changing stress distribution inside these complete but not absolutely homogeneous infiltrated hip joint heads resulted in lower strength compared to gradient hip joint heads.

As expected, the examined samples B and C showed an increasing average density proportional to the average Y_2O_3 stabilized zirconia content (Table 3).

At least 10 samples of each charge A (Bionit®), B and C underwent burst load testing in accordance with ISO 7206-10 CoCr test spigots. With 60 kN, the burst load of the 5 times fully infiltrated samples (series B) was by 27% higher than the burst load of the Al_2O_3 samples (Bionit®) with 47 kN (Fig. 12). But highest values were achieved by the partially infiltrated samples (infiltrated only 3 times on one side) from series C with a burst load of 66 kN. This corresponds to an increase of 41% compared to samples A (Bionit®). A high Y_2O_3 stabilized zirconia gradient in alumina may result in different shrinkage in small volumes of material and resulted, microstructure damage and decreasing strength. That is discussed correspondingly in particular results below.

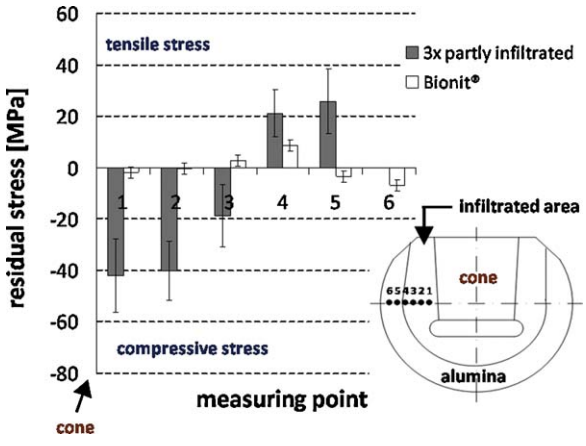

Fig. 11. Residual stress distribution on fracture surfaces of Bionit® (alumina) hip joint head and a one side infiltrated graded Y_2O_3 stabilized zirconia alumina composite hip joint head.

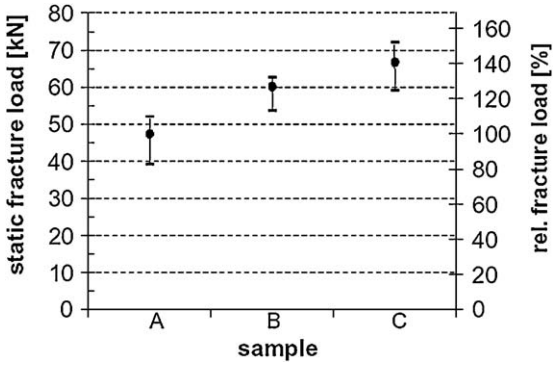

Fig. 12. Average, minimum and maximum fracture strength of the samples A (Bionit®), B and C after sintering and finishing.[19,20]

Both disc-form samples and hip joint heads from Al_2O_3 showed significantly higher strength after infiltration with Y_2O_3 stabilized zirconia salts and subsequent sintering. Microstructure approved that result. The pure Al_2O_3 ceramic Bionit® (Fig. 13) had a homogenous fine microstructure with medium grain size of about 2.4 μm. In the case of grinding and SEM analysis (electron back scattering) for each partially infiltrated hip joint head, the Y_2O_3 stabilized zirconia was able to be identified in the infiltration area as a separate dispersion in the grain boundary pendentives of the Al_2O_3 grains (Figs. 14 and 15). The separate Y_2O_3 stabilized zirconia consisted almost exclusively of tetragonal and cubic stabilized ZrO_2 in accordance with the XRD investigation. Furthermore, compared to the non-infiltrated Al_2O_3 ceramic Bionit® which showed an average alumina grain size of 2.4 μm, a significant (U_{test} according to Wilcox, Mann and Whitney with 5% significance level) greater reduction of the grain size of the Al_2O_3 matrix grains was observed. In the process, it was found that with higher Y_2O_3

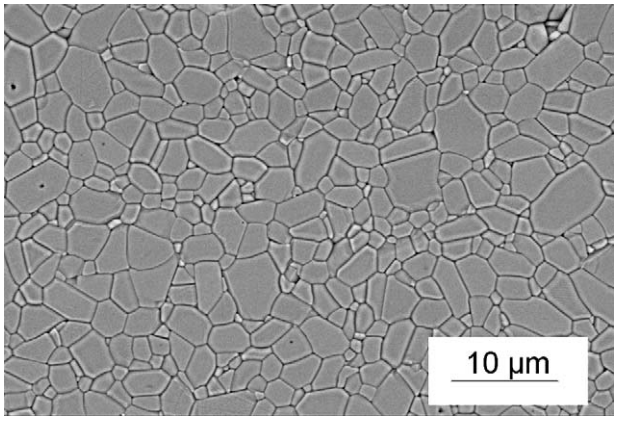

Fig. 13. SEM image from series A – Al_2O_3 (Bionit®).

Table 4
Medium grain size on infiltrated and sintered Al_2O_3 hip joint balls.

Sample	Number of infiltrations	Medium grain size	[μm]
A (Bionit®)	–	Al_2O_3	2.4
B	5 times fully	Al_2O_3	0.61
		Y_2O_3 stabilized ZrO_2	0.39
C	3 times partially	Al_2O_3	0.78
		Y_2O_3 stabilized ZrO_2	0.39

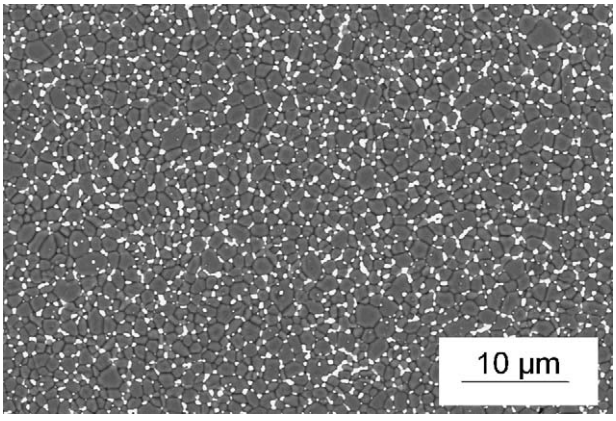

Fig. 14. SEM image from series C – area infiltrated 3 times.

stabilized zirconia content, finer microstructures were able to be created – as can be seen from comparing Fig. 15 (∼17 wt% Y_2O_3 stabilized zirconia in the conical area) with Fig. 14 (∼12 wt% Y_2O_3 stabilized zirconia in the conical area). Consequently, the smallest average grain size of 0.61 μm for the alumina grains with Y_2O_3 stabilized zirconia content of ∼17 wt% was found for the hip joint heads of series B (Table 4).

In Table 4 the determined medium grain sizes of all investigated hip joint heads are summarized. The separated Y_2O_3 stabilized zirconia acted as an inhibitor to grain growth during sintering. The higher strength of the Al_2O_3 ceramic infiltrated with Y_2O_3 stabilized zirconia is therefore based (a) on a transformation toughening mechanism (3.2), thus the crack arborization through the phase transformation of the Y_2O_3 stabilized zirconia and (b) on the microstructure refinement through growth inhibiting Y_2O_3 stabilized zirconia particles.[12]

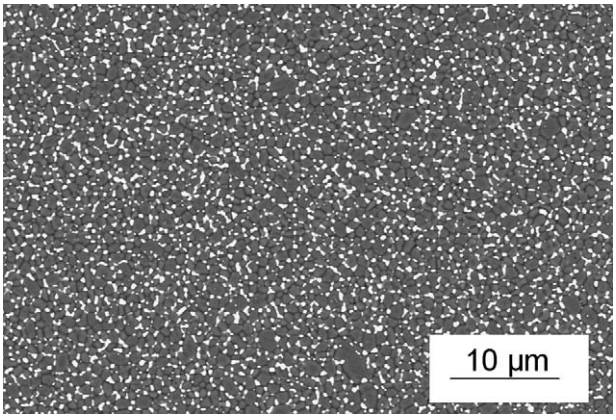

Fig. 15. SEM image from series B – area infiltrated 5 times.

Fig. 16 shows the FEM stress distribution of a non-infiltrated hip joint head on loading. Tensile stresses in the area of the conical bore of the hip joint head lead to bursting. During the fracture strength investigation of infiltrated hip joint heads, the partially infiltrated samples (samples C) showed significantly greater fracture strength than the fully infiltrated samples (samples B). In the process, the entire Y_2O_3 stabilized zirconia content of samples C was lower than that of samples B. For local ZrO_2 dispersion, practically identical, maximum ZrO_2 content was found for both sample loads. The sinter shrinkage was measured on the fully infiltrated discs (samples 0–V). Here (Fig. 17) it was found that the sinter shrinkage linearly reduced with increasing Y_2O_3 stabilized zirconia proportion from 16.3% (sample 0, pure Al_2O_3) to 12.7% (sample V). In the case of the hip joint heads infiltrated on one side (series C), a smaller shrinkage in the conical area appeared during sintering than in the remaining, non-infiltrated component, which led to low compression stress in the conical area. At the same time, a formation of low tensile stress occurred in the non-infiltrated area. The created stress relationships (but only low values) proved to be positive for behavior under the effect of loading. During the burst load

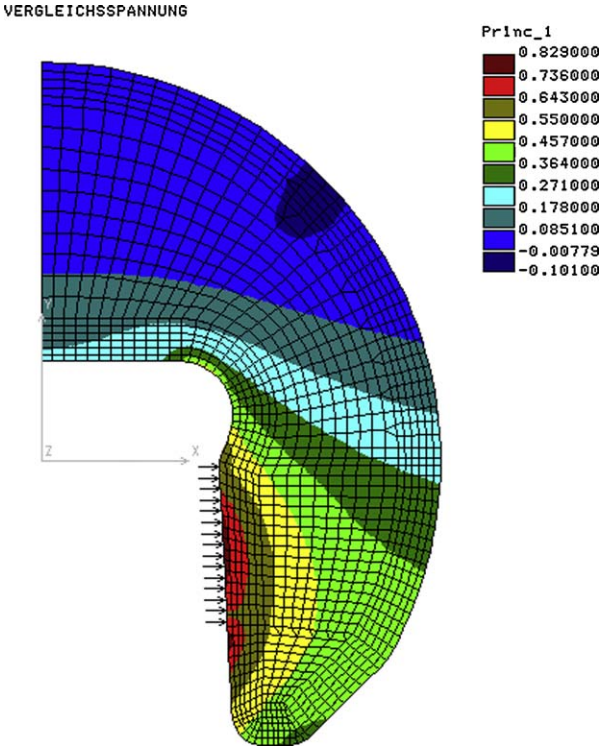

Fig. 16. Stress distribution in a hip joint head on load application.

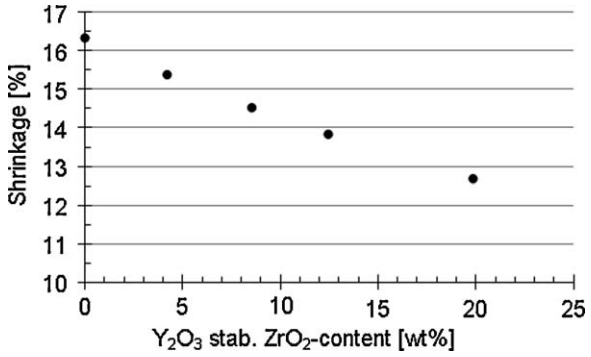

Fig. 17. Linear shrinkage of samples 0, I, II, III and V (fully infiltrated b-discs).

investigation, component failure occurred through tensile loading in the conical area. The compression stress existing in the graded material partly counterbalanced the tensile loading during the burst loading testing, whereby an increase in the burst load was achieved.[19] Related behavior was observed by Novak preparing gradient material layer by layer.[7]

In addition to the transformation toughening and microstructure refinement mechanisms described, in the case of one-sided infiltrated Al_2O_3 hip joint balls, the increase in fracture strength is based on a partial compensation of stress. The stress relationships in the infiltrated and non-infiltrated area of the graded material have to be furthermore critically evaluated in further studies to ensure safeness of gradient ceramic implants.

4. Conclusions

Infiltration of porous alumina bodies with Y_2O_3 and ZrO_2 salt solution is possible. By drying, and thermal treatments (1000 °C, sintering, HIP) ZTA dispersion ceramics can be generated. Via this process, stabilized ZrO_2 with low monocline content succeeds in a unique homogeneous dispersion in the grain boundary pendentives of the Al_2O_3 ceramic and a consistently improved Al_2O_3 microstructure results through the grain growth hindering effect of the ZrO_2. ZTA ceramics manufactured in this way showed significantly higher fracture strength than pure Al_2O_3 ceramic due to the dispersion ceramic itself, the transformation toughening and microstructure refinement mechanisms without a negative impact on their wear properties.

However, the process of salt infiltration also enables the formation of Y_2O_3 stabilized zirconia gradients in an Al_2O_3 matrix through one-sided infiltration. Due to the varying shrinkage of ZTA and Al_2O_3, stresses arise in ceramic components which partly counterbalance the loaded tension expected, probably leading to a further increase in fracture strength. But the relationships inside a gradient composite are complex and require further studies according to microstructure and stress distribution. First evaluation of residual stress on a fractured surface showed low compressive stress in infiltrated cone area. Further evaluation of the stress relationships in the graded ceramics will be the subject of further investigations. Thereby different methods (XRD, neutron diffraction and synchrotron radiation) and different sample surfaces as well as a meaningful investigation method for large surfaces and volumes as implant components have, should be used or have to be developed.

Salt infiltration does not only represent a simple process for the production of ZTA ceramics, but it also offers the possibility of the targeted insertion of material and microstructure gradients in Al_2O_3 ceramics. Therefore, pre-stressed components with high fracture strength can be produced in a simple way. Despite all the concerns the homogeneous and graded ZTA dispersion ceramics presented here constitute a potential bioceramic material for use in the manufacture of novel load-bearing joint implant components.

Acknowledgment

We would like to thank the German Federal Ministry of Education and Research (BMBF) for financially supporting the project (project funding reference no. 03WKF23B).

References

1. Willmann G. Alumina ceramic looks back 20 years of use in medical applications. *Biomed Tech* 1994;**39**(4):73–8.
2. Rieger W. Ceramics in orthopedics – 30 years of evolution and experience. In: Rieker C, Oberholzer S, Wyss U, editors. *World tribology forum in arthroplasty proceedings*. Bern: Hans Huber; 2001. p. 283–94.
3. Begand S, Oberbach T, Glien W. Investigations of the mechanical properties of an alumina toughened zirconia ceramic for an application in joint protheses. *Key Eng Mater* 2005;**284–286**:1019–22.
4. Clarke IC, Pezzotti G, Green DD, Shirasu H, Donaldson T. Severe simulation test for run-in wear of all-alumina compared to alumina composite THR. In: D'Antonio JA, Dietrich M, editors. *Bioceramics and alternative bearings in joint arthroplasty*. Darmstadt: Steinkopf; 2005. p. 11–20.
5. Anné G, Vanmeensel K, Vleugels J, Van der Biest O. Electrophoretic deposition as a novel near net shaping technique for functionally graded biomaterials. *Key Eng Mater* 2006;**314**:213–8.
6. Anné G, Hecht-Mijic S, Richter H, Van der Biest O, Vleugels J. Strength and residual stresses of functionally graded Al_2O_3/ZrO_2 discs prepared by electrophoretic deposition. *Scripta Mater* 2006;**54**:2053–6.
7. Novak S, Kalin M, Lukas P, Anne G, Vleugels J, Van der Biest O. The effect of residual stresses in functionally graded alumina–ZTA composites on their wear and friction behaviour. *J Eur Ceram Soc* 2007;**27**:151–6.
8. Low IM. Infiltration processing of novel layered and graded materials. In: Khor KA, Srivarsan TS, Moore JJ, editors. *Proceedings of international symposium on processing and fabrication of advanced materials VI*. 1998. p. 1971–84.
9. Honeyman CP, Lange FF. Infiltration of porous alumina bodies with solution precursors: strengthening via compositional grading, grain size control and transformation toughening. *J Am Ceram Soc* 1996;**79**(7):1810–4.
10. Naslain R, Langlais F, Vignoles G, Pailler R. The CVI-process. State of the art and perspective. In: Tandon R, Wereszczak A, Lara-Curzio E, editors. *Mechanical properties and performance of engineering ceramics. II: ceramic engineering and science proceedings, 27(2)*. Hoboken, NJ, USA: John Wiley & Sons Inc.; 2008. p. 373–8, doi:10.1002/9780470291313.ch37.
11. Galusek G, Majling J. Preparation of Al_2O_3–ZrO_2 ceramics by infiltration processing. *Ceram Int* 1995;**21**(2):101–7.
12. Riou S, Queroux F, Boch P. Zirconia–alumina particulate composites by infiltration processing. *Ceram Int* 1995;**21**(5):339–43.
13. Asmi D, Low I. Processing of an in-situ layered and graded alumina/calcium–hexaluminate composite: physical characteristics. *J Eur Ceram Soc* 1998;**18**(14):2019–24.
14. Singh M, Low I, Layered. graded alumina-based hybrid composites by infiltration processing. *Key Eng Mater* 2002;**224–226**:493–8.

15. Pratapa S, Low I, O'Connor B. Infiltration processed, functionally graded aluminium titanate/zirconia–alumina composite. Part I: microstructural characterization and physical properties. *J Mater Sci* 1998;**33**(12):3037–45.
16. Ortmann C, Oberbach T, Glien W, Richter H, Puhlfürß P. Alumina with zirconia gradient – innovative bioceramics. In: Heinrich JG, S Aneziris CG, editors. *Proceedings of 10th international conference of ECERS*. Baden-Baden: Göller Verlag GmbH; 2008., ISBN 3-87264-022-4 p. 995–8.
17. ISO 7206-10. *Implants for surgery – partial and total hip-joint prostheses – determination of resistance to static load of modular femoral heads*; 2003, ISBN 0580431169.
18. ISO 6474. *Implants for surgery – ceramic materials based on high purity alumina*; 1994. ICS 11.040.40.
19. Ortmann C, Oberbach T, Richter H, Puhlfürß P. Wear screening of ZTA dispersion ceramics. In: Bucko MM, Haberko K, Pedzich KZ, Zych L, editors. *Proceedings of 11th international conference of ECERS, Polish ceramic society*. 2010., ISBN 978-83-60958-45-2 p. 396–9.
20. Oberbach T, Begand S, Glien W, Kaddick C. Tribological behaviour of different ceramics in the system Al_2O_3–ZrO_2. In: Heinrich JG, Aneziris CG, editors. *Proceedings of 10th international conference of ECERS*. Baden-Baden: Göller Verlag GmbH; 2008. ISBN: 3-87264r-r022-4.